Metal–Organic Frameworks

DOI: 10.1002/ange.200901177

Nanoporous Nanorods Fabricated by Coordination Modulation and Oriented Attachment Growth**

*Takaaki Tsuruoka, Shuhei Furukawa, Yohei Takashima, Kaname Yoshida, Seiji Isoda, and Susumu Kitagawa**

Well-designed metal–organic hybrid porous materials—so-called porous coordination polymers (PCPs) or metal–organic frameworks (MOFs)—can be made from an assembly of organic linkers with metal ions.[1–6] This class of materials was recently recognized as an intriguing class of crystalline nanoporous materials for gas sorption, separation, and catalysis because their framework topologies and pore sizes can be designed for selective guest accommodation, and the functionality of the pore surfaces directly influences the interaction with guest molecules. Miniaturizing the size of PCP crystals to the nanometer scale[7–10] by functionalizing the crystal interfaces will provide further opportunities to integrate novel functions into the materials without changing the characteristic features of the PCP crystal itself, and will allow the correlation between the porous properties and interfacial structures of nanocrystals to be investigated. Despite the advantages of nanosized PCPs, growth processes that are most important in establishing a universal methodology for the creation of nanosized PCPs are still unclear because there is no suitable defining protocol.[7,10–13] Understanding the crystal growth of framework materials, moreover, promises to determine the fundamental requirements of bottom-up self-assembly processes. Herein, we show that a simple but straightforward method using capping reagents that perturb the framework extension of PCPs can be applied to determine their crystal features. We describe the tetragonal framework system of PCP nanorods defined by selectively modulating the coordination interaction in the framework, which enhances the one-dimensional anisotropic fusion of the cubic nanocrystals, indicating an oriented attachment mechanism.[14,15] Moreover, the correlation between the sorption properties and crystallinity of the nanorods shows that the coordination modulation method can produce highly crystalline nanorods with high porosity comparable to that of bulk crystals synthesized by using the conventional solvothermal method.

The relatively weak interactions of the coordination bonds dominate the hierarchical self-assembly process involved in constructing the sparse three-dimensional porous frameworks of PCPs with nanometer lattice constants, leading to the formation of crystals. This feature distinguishes this class of molecular-based materials from dense inorganic materials, such as metal[16] and semiconductor crystals,[17] and from conventional porous materials such as zeolites[18,19] and mesoporous silica.[20,21] Controlling the interactions between metal ions and organic linkers, so-called "coordination equilibria", is important when varying the crystal features of PCPs, such as their size, morphology, and crystallinity. Although several approaches have been developed to fabricate PCP nanoparticles, such as reversed micelles[22] and microwave-assisted methods,[23,24] the crystal-growth mechanism has rarely been discussed because it is difficult to control the rate of framework extension.[25] Our strategy, inspired by the method to fabricate metal or semiconductor nanoparticles[26,27] and by the preliminary work done by Fischer and coworkers,[7] is to modulate the coordination equilibria simply by adding capping reagents (modulators) with the same chemical functionality as the linkers, to impede the coordination interaction between the metal ions and the organic linkers, which generates a competitive situation that regulates the rate of framework extension and crystal growth (Scheme 1). The selective modulation of the coordination interactions allows us to control the resulting crystal morphology, which reflects the framework symmetry based on the anisotropic coordination mode.

The three-dimensional porous coordination framework $[\{Cu_2(ndc)_2(dabco)\}_n]$[28] (**1**; ndc = 1,4-naphthalene dicarboxylate; dabco = 1,4-diazabicyclo[2.2.2]octane) has a tetragonal crystal system ($P4/mmm$, $a = 10.8190(3)$ Å, $c = 9.6348(6)$ Å), in which the dicarboxylate layer ligands (ndc) link to the dicopper clusters to form two-dimensional square lattices, which are connected by amine pillar ligands (dabco) at the lattice points (Figure 1 a,b).[28–32] Hence, **1** is a good compound with which to investigate the crystal growth mechanisms of

[*] Dr. T. Tsuruoka, Dr. S. Furukawa, Prof. S. Kitagawa
ERATO Kitagawa Integrated Pores Project
Japan Science and Technology Agency (JST)
Kyoto Research Park Bldg #3, Shimogyo-ku, Kyoto 600-8815 (Japan)
Fax: (+81) 75-325-3572
E-mail: kitagawa@sbchem.kyoto-u.ac.jp
Homepage: http://kip.jst.go.jp
Dr. S. Furukawa, Prof. S. Kitagawa
Institute for Integrated Cell-Material Sciences (iCeMS), Kyoto University
Yoshida, Sakyo-ku, Kyoto 606-8501 (Japan)
Y. Takashima, Prof. S. Kitagawa
Department of Synthetic Chemistry & Biological Chemistry
Graduate School of Engineering, Kyoto University
Katsura, Nishikyo-ku, Kyoto 615-8510 (Japan)
Dr. K. Yoshida, Prof. S. Isoda
Institute for Chemical Research, Kyoto University
Uji, Kyoto 611-0011 (Japan)

[**] Part of this work was conducted in the Kyoto Advanced Nanotechnology Network, supported by the "Nanotechnology Network" of the Ministry of Education, Culture, Sports, Science and Technology (MEXT) (Japan). We acknowledge Dr. Daisuke Tanaka for fruitful discussion.

Supporting information for this article is available on the WWW under http://dx.doi.org/10.1002/anie.200901177.

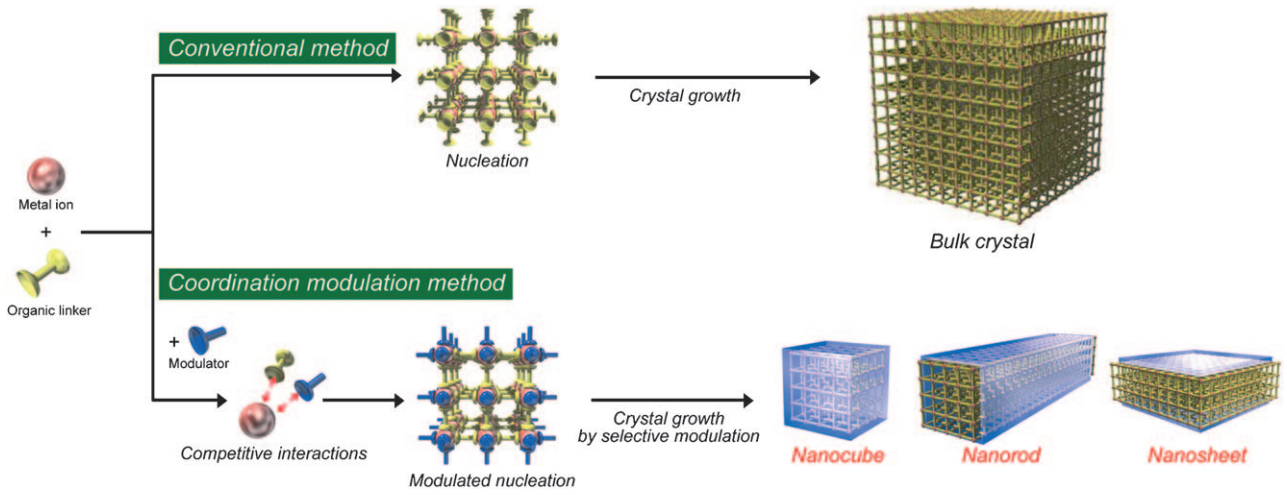

Scheme 1. Coordination modulation method for fabricating porous coordination polymer (PCP) nanocrystals. Modulated nucleation is induced by the addition of modulators with the same functionality as organic linkers to impede the coordination interaction between metal ions and organic linkers. Selective coordination modulation in one of the coordination modes (illustrated as blue shells) to construct the framework then leads to anisotropic growth of the PCP crystals.

PCPs. The anisotropic framework feature of **1**, dominated by two coordination modes (ndc–copper and dabco–copper), allows the selective modulation of one of the coordination modes (ndc–copper) by adding a monocarboxylic acid as the modulator. The modulator can also physically prevent the aggregation of crystals, which leads to anisotropic growth. Nanocrystals of **1** were synthesized by adding a solution of 1,4-naphthalenedicarboxylic acid (ndcH, 0.06 M) and dabco (0.03 M) in dimethylformamide (DMF) to a solution of copper acetate (0.06 M) in DMF in the presence of 0.6 M acetic acid at 100 °C for 24 h. In this set of experiments, these concentrations are defined as the standard conditions.

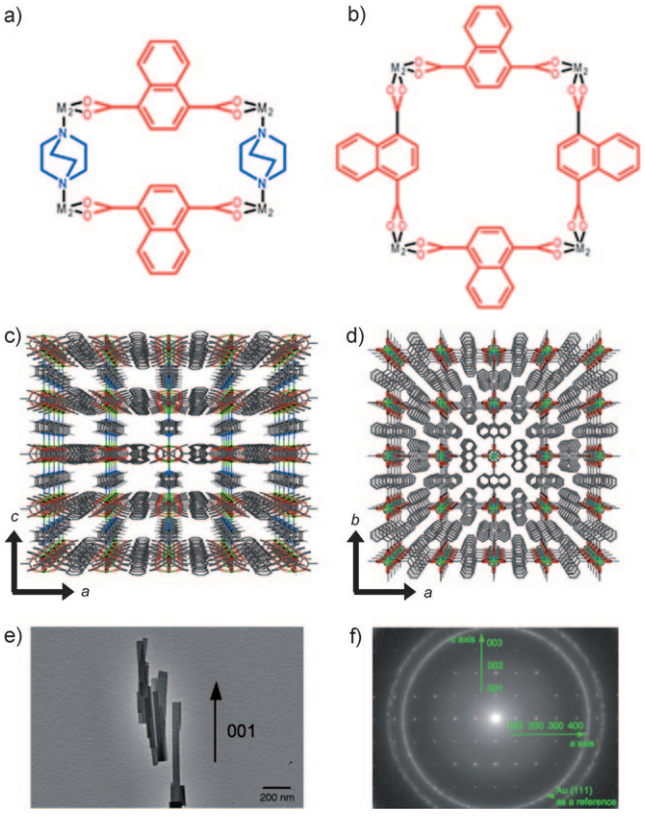

Figure 1. Crystal structure of $[\{Cu_2(ndc)_2(dabco)\}_n]$ and its appearance as nanocrystals. a,b) The chemical structures of a) the (100) surface and b) the (001) surface. c,d) The crystal structure of $[\{Cu_2(ndc)_2(dabco)\}_n]$ viewed along the c) *b* axis and the d) *c* axis. The naphthalene moieties are disordered owing to the symmetry. e) Typical TEM image of $[\{Cu_2(ndc)_2(dabco)\}_n]$ nanocrystals obtained after reaction for 24 h at the standard conditions. f) Electron diffraction pattern from a single nanorod.

The transmission electron microscopy (TEM) image of **1** clearly shows the anisotropic growth of the nanocrystals (Figure 1 c). The average lengths of the major and minor axes are 392 ± 210 and (82 ± 23) nm, respectively. Nanocrystals with a square-rod morphology, which thus form nanorods, were identified by cross-sectional analysis of the atomic force microscopy images (Supporting Information, Figure S1), in which the heights of the nanocrystals (ca. 70 nm) corresponded to the minor axis rather than to the major axis. The electron diffraction pattern of individual nanorods of **1** (Figure 1 d) revealed a correlation between the anisotropic crystal morphology and the tetragonal framework system; the major axis of the nanorod was coincident with the [001] direction of the framework. Therefore, the coordination mode of dabco–copper in the [001] direction is the more preferable interaction for crystal growth than the coordination mode of ndc–copper in the [100] direction. The ndc–copper interaction, which forms the two-dimensional layer, was impeded by the presence of acetic acid as the modulator because both ndc and acetate have the same carboxylate functionality. Therefore, the selective coordination modulation method enhanced the relative crystal growth in the [001] direction.

To clarify the effect of the modulator on the mechanisms of framework construction and crystal growth, the concentration of acetic acid was altered across the range 0–1.0 M, while the rest of the standard conditions were maintained. Whereas a green precipitate was immediately formed at the

lower concentrations (less than 0.4 M), the addition of large amounts of acetic acid (greater than 0.6 M) induced a slow reaction to produce the green precipitate: 20 min for 0.6 M, 1 h for 0.8 M, and 3 h for 1.0 M. The subtle morphology of the aggregated crystals was observed by TEM of samples prepared with acetic acid concentrations below 0.4 M. Individual nanorods were clearly resolved and the aspect ratio (major axis/minor axis) of the nanorods increased with the concentration of acetic acids from 0.6 to 1.0 M (Supporting Information, Figure S2). The increase in the acetic acid concentration significantly decelerated the rate of crystal growth and facilitated the formation of nanorods with high aspect ratios by inhibiting growth in the [100] direction.

Interestingly, the X-ray diffraction (XRD) patterns of the green precipitate had sharp diffraction peaks for the nanorods, in contrast to the broader diffraction peaks for the aggregated crystals prepared in the acetic acid solutions of lower concentrations (Figure 2a). The rapid crystal growth of **1** (at concentrations of acetic acid below 0.4 M) induced a less-crystalline framework, because the procedure described herein is not suitable for producing bulk powder samples of **1**, which are generally synthesized at higher temperature by the conventional two-step solvothermal method.[30] The adsorption isotherms for nitrogen and carbon dioxide of highly crystalline nanorods prepared with 0.6 M acetic acid and less-crystalline aggregated crystals prepared without acetic acid clearly indicate the amounts of nitrogen and carbon dioxide adsorbed by the nanorods were significantly more than amounts adsorbed by the aggregated crystals and were almost comparable to amounts adsorbed by the bulk powders prepared using the solvothermal method.[32] The lower sorption amount of the aggregated crystals is most likely attributed to the lower crystallinity and critical number of defects that can block the channels. The competitive interaction of the ndc–copper and the acetate–copper is essential to reduce the reaction rate in constructing a framework with high crystallinity and in growing anisotropic nanocrystals.

Great insight into the anisotropic crystal growth of **1** can be gained from an analysis of the time course of the reaction under the standard conditions by TEM. After a reaction time of 15 min, only nanoparticles with an average diameter of 4.9 ± 0.9 nm were observed (Figure 3a), which can be considered the nucleation stage of crystal growth. After a reaction time of 20 min, cubic nanocrystals with a size of 77 ± 13 nm started to become visible (Figure 3b), together with 5 nm nanoparticles. Nanorods with a high aspect ratio were observed after a reaction time of 30 min. Note that the length of the nanorods in the [001] direction increased with increasing reaction times up to 24 h. In contrast, the average width of the nanorods, which corresponded to the size of the nanocubes did not change significantly as the reaction time increased (Supporting Information, Figure S3 and Table S1). The numbers of each nanoobject (nanoparticles, nanocubes, and nanorods) were counted on TEM images (Figure 3d). In the initial stage of the reaction (up to 1 h), the number of nanocubes decreased with a simultaneous increase in the number of nanorods. After a reaction time of 2 h, the numbers of nanocubes and nanorods were almost constant. In contrast,

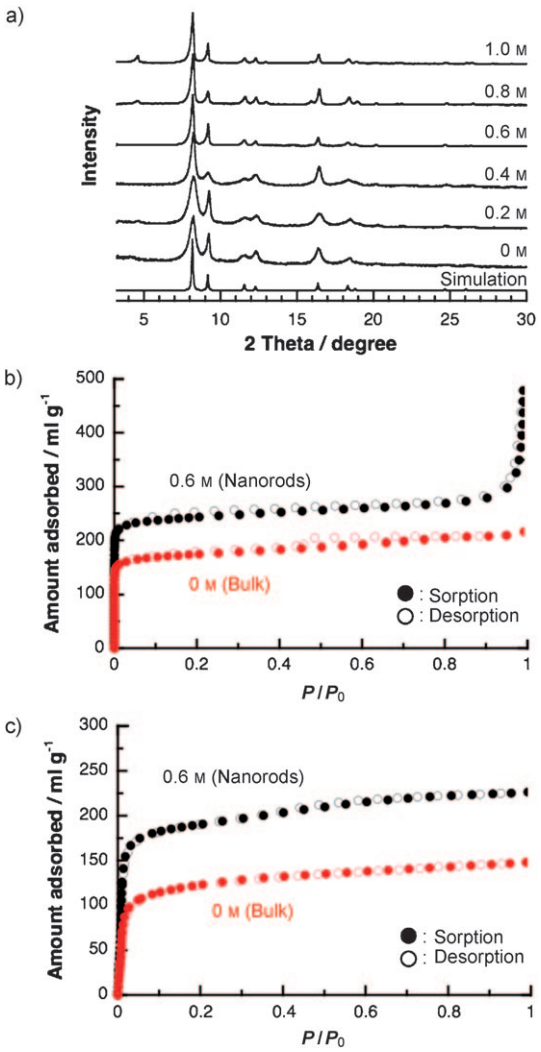

Figure 2. a) Changes in the crystallinity of $[\{Cu_2(ndc)_2(dabco)\}_n]$ frameworks as a function of concentration of acetic acid molecules. Simulated and observed XRD patterns of $[\{Cu_2(ndc)_2(dabco)\}_n]$ frameworks prepared by the different concentrations of acetic acid (0.0–1.0 M). Gas adsorption isotherms of b) nitrogen at 77 K and c) carbon dioxide at 195 K for $[\{Cu_2(ndc)_2(dabco)\}_n]$ bulk powders prepared without acetic acid (red) and nanorods prepared with 0.6 M acetic acid (black).

the number of nanoparticles did not change during the whole course of the reaction.

On the basis of these results, we propose a growth mechanism for the nanorods of **1** (Scheme 2). Nanoparticles with a size of around 5 nm, including the framework components, form in the early stage of the reaction, when a maximum of 125 framework units can be constructed. This stage is followed by the formation of nanocubes with an average size of around 80 nm. The generation of 80 nm nanocubes is based on the fusion of the nanoparticles, because no object of intermediate size has ever been observed. The formation of the nanocubes requires a threshold number of nanoparticles, which is indicated by two lines of evidence: the constant number of nanoparticles during the whole reaction and the fact that the residue filtered after a reaction time of 24 h never produced nanocubes, even when heated again at

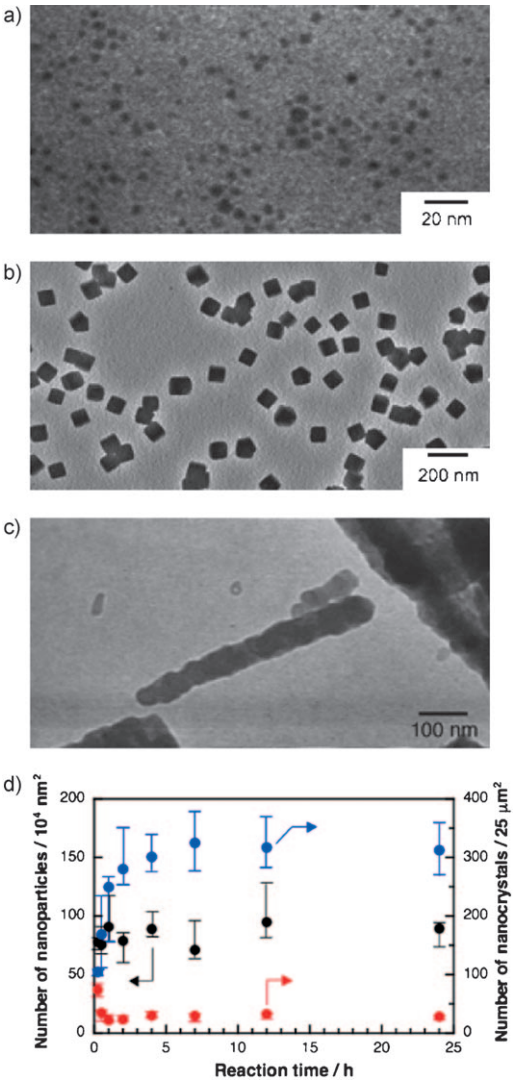

Figure 3. Time-course analysis of the reaction under the standard conditions. TEM images of [{$Cu_2(ndc)_2(dabco)$}$_n$] nanocrystals obtained after reaction times of a) 15 min, b) 20 min, and c) 1 h. d) Changes in the number of nanoparticles (black), nanocubes (red), and nanorods (blue) as a function of reaction time.

100 °C for 5 days. The nanorods grow by the oriented attachment of the nanocubes by collision of nanocubes in solution,[33–35] because the width of the nanorods is almost constant at 80 nm, corresponding to the size of the nanocubes. The observation of nanorods with rough surfaces (Figure 3c) and the stepwise increase in the aspect ratio (Supporting Information, Figure S4) is key evidence of oriented attachment growth. Although direct experimental evidence that acetic acid molecules bind to the surfaces of nanocube and nanorods has not been obtained, the four surfaces of nanorods, (100), ($\bar{1}$00), (010), and (0$\bar{1}$0), are influenced by acetic acid modulators to suppress the fusion of the nanocubes in the [100] direction. Therefore, the anisotropic growth from the nanocubes to the nanorods accrues by the connection with the dabco linkers to the (001) and (00$\bar{1}$) surfaces, where the modulation effect is rather less significant.

This mechanism is also supported by the observation that the length of the nanorods depends on the concentrations of all starting materials and on maintaining the molar ratio of the standard conditions (Supporting Information, Figure S5). Halving the concentration of the standard condition resulted in a longer reaction time to obtain precipitation (ca. 40 min), which indicates slower formation of the nanorods. Whereas the lengths of the resulting nanorods decreased after a reaction time of 24 h, the widths corresponded to those of nanorods prepared under the standard conditions. Doubling the concentration of all starting materials produced longer nanorods with the same width. This result can be explained by the higher concentration of all starting materials providing a larger number of nanocubes, resulting in the higher probability of crystal collision to elongate the nanorods. These experiments provide evidence for crystal growth by the oriented attachment mechanism.

In summary, we demonstrated that a coordination modulation method, in which acetic acid is used to directly influence the coordination equilibria, can be used to control the crystal growth of nanosized PCP crystals [{$Cu_2(ndc)_2$-(dabco)}$_n$]. The competitive interaction between the coordination mode used to construct the framework and the acetate–copper interaction plays a crucial role in determining the reaction rate and crystal morphology. The mechanism of anisotropic crystal growth is clearly explained by oriented attachment. The coordination modulation method affords perfect framework regularity in PCP nanocrystals, which allows the nanocrystals to be applied as crystalline porous materials. This methodology promises universality in controlling the crystal growth of a variety of PCPs because most PCPs are constructed with dicarboxylate linkers. This work should open the way

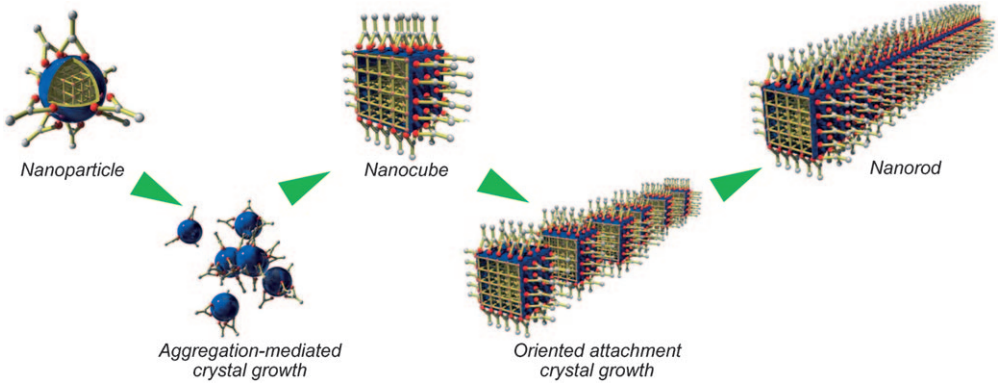

Scheme 2. Proposed growth mechanism for [{$Cu_2(ndc)_2(dabco)$}$_n$] nanorods. The growth process of nanocubes is a consequence of nanoparticle aggregation-mediated crystal growth. The selective coordination modulation on the (100) surfaces of the nanocubes induces the oriented attachment leading the growth of nanorods in the [001] direction. Although direct information on the surface structures of nanocubes and nanorods has not been obtained, one of the plausible and also possibly dynamic surface structures is shown.

to the fabrication of nanosized PCP materials for more advanced applications.

Experimental Section

Nanocrystals of **1** were prepared by the coordination modulation method. A solution of $Cu(OCOCH_3)_2{\cdot}H_2O$ (0.06 M) and CH_3COOH (0.6 M) in DMF (15 mL) was heated at 100 °C in a two-necked flask. When the temperature of the copper solution reached to 100 °C, a solution of ndcH (0.06 M) and dabco (0.03 M) in DMF (10 mL) was added to the copper solution. After the reaction had run for 24 h, the resulting samples were filtered through a 0.2 μm membrane filter, washed with DMF several times, and dried using a vacuum pump.

The TEM observations were performed with a JEOL JEM-2000 transmission electron microscope operating at 120 kV. The TEM samples of the final products obtained after reaction for 24 h were prepared by dispersing the green precipitates in toluene, and then dropping the solution onto a carbon-coated TEM grid. For the time-course TEM observations of the reaction, aliquots with a needle-tip amount of the reaction solution were removed at each time point and dropped onto a carbon-coated TEM grid. The size and size distribution of nanocrystals were measured using calibrated TEM images by ImageJ software (a public domain image processing and analysis program). The numbers of nanocrystals (nanoparticles, nanocubes, and nanorods) for Figure 3d were estimated by using the TEM images as follows. In the case of counting the averaged numbers of nanocubes and nanorods, 10 TEM images with an area of 25 μm^2 were used. For the nanoparticles counting, 10 TEM images with an area of 10000 nm^2 were used.

Atomic force microscopy images were obtained on a Pico-plus 5500 SPM instrument (Agilent Technologies) operating in a dynamic-force microscopic mode. A silicon cantilever (Olympus) with a force constant $K \approx 3\ N\,m^{-1}$ and a resonance frequency of approximately 80 kHz was used. The sample was prepared by dropping the toluene solution (described in the TEM section) onto a freshly cleaved HOPG surface and allowing it to evaporate at room temperature.

The sorption isotherms of bulk and nanorods for nitrogen at 77 K and carbon dioxide at 195 K were recorded on a BELSORP-max volumetric-adsorption instrument from BEL Japan, Inc. All measurements were performed using the samples after pretreatment at 100 °C under vacuum conditions.

Crystallographic analysis of an individual nanorod was carried out by electron diffraction crystallography. Electron diffraction patterns were taken with a transmission electron microscope (JEOL JEM2000FX-II) at an accelerating voltage of 200 kV. To obtain electron diffraction patterns, samples were placed on an electron microscopic microgrid reinforced by gold and amorphous carbon. The relation between crystallographic orientation and morphology was estimated from the diffraction net pattern and corresponding image.

X-ray powder diffraction data were collected on a Rigaku RINT-2200 Right System (Ultima IV) diffractometer with $Cu_{K\alpha}$ radiation. The simulated pattern was obtained from single-crystal X-ray analysis.

Received: March 2, 2009
Revised: April 14, 2009
Published online: May 26, 2009

Keywords: coordination modes · coordination polymers · crystal growth · nanostructures

[1] O. M. Yaghi, M. O'Keeffe, N. W. Ockwig, H. K. Chae, M. Eddaoudi, J. Kim, *Nature* **2003**, *423*, 705 – 714.
[2] S. Kitagawa, R. Kitaura, S. Noro, *Angew. Chem. Int. Ed.* **2004**, *43*, 2334 – 2375.
[3] G. Férey, C. Mellot-Draznieks, C. Serre, F. Millange, *Acc. Chem. Res.* **2005**, *38*, 217 – 225.
[4] U. Mueller, M. Schubert, F. Teich, H. Puetter, K. Schierle-Arndt, J. Pastré, *J. Mater. Chem.* **2006**, *16*, 626 – 636.
[5] B. D. Chandler, G. D. Enright, K. A. Udachin, S. Pawsey, J. A. Ripmeester, D. T. Cramb, G. K. H. Shimizu, *Nat. Mater.* **2008**, *7*, 229 – 235.
[6] M. Dinca, J. R. Long, *Angew. Chem. Int. Ed.* **2008**, *47*, 6766 – 6779.
[7] S. Hermes, T. Witte, T. Hikov, D. Zacher, S. Bahnmüller, G. Langstein, K. Huber, R. A. Fischer, *J. Am. Chem. Soc.* **2007**, *129*, 5324 – 5325.
[8] W. Lin, W. J. Rieter, K. M. L. Taylor, *Angew. Chem. Int. Ed.* **2009**, *48*, 650 – 658.
[9] A. M. Spokoyny, D. Kim, A. Sumrein, C. A. Mirkin, *Chem. Soc. Rev.* **2009**, *38*, 1218 – 1227.
[10] D. Zacher, J. Liu, K. Huber, R. A. Fischer, *Chem. Commun.* **2009**, 1031 – 1033.
[11] M. Shoaee, M. W. Anderson, M. P. Attfield, *Angew. Chem. Int. Ed.* **2008**, *47*, 8525 – 8528.
[12] K. Szelagowska-Kunstman, P. Cyganik, M. Goryl, D. Zacher, Z. Puterova, R. A. Fischer, M. J. Szymonski, *J. Am. Chem. Soc.* **2008**, *130*, 14446 – 14447.
[13] R. E. Morris, *ChemPhysChem.* **2009**, *10*, 327 – 329.
[14] H. Cölfen, M. Antonietti, *Mesocrystals and Nonclassical Crystallization*, John Wiley & Sons, Chichester, **2008**.
[15] H. Cölfen, S. Mann, *Angew. Chem. Int. Ed.* **2003**, *42*, 2350 – 2365.
[16] Y. Xia, P. Yang, Y. Sun, Y. Wu, B. Mayers, Y. Gates, Y. Yin, F. Kim, H. Yan, *Adv. Mater.* **2003**, *15*, 353 – 389.
[17] C. Burda, X. Chen, R. Narayanan, M. A. El-Sayed, *Chem. Rev.* **2005**, *105*, 1025 – 1102.
[18] T. Bein, *Chem. Mater.* **1996**, *8*, 1636 – 1653.
[19] M. E. Davis, *Nature* **2002**, *417*, 813 – 821.
[20] A. Sayari, S. Hamoudi, *Chem. Mater.* **2001**, *13*, 3151 – 3168.
[21] F. Hoffmann, M. Cornelius, J. Morell, M. Fröba, *Angew. Chem. Int. Ed.* **2006**, *45*, 3216 – 3251.
[22] W. J. Rieter, K. M. L. Taylor, H. An, W. Lin, W. Lin, *J. Am. Chem. Soc.* **2006**, *128*, 9024 – 9025.
[23] Z. Ni, R. I. Masel, *J. Am. Chem. Soc.* **2006**, *128*, 12394 – 12395.
[24] L.-G. Qiu, Z.-Q. Li, Y. Wu, W. Wang, T. Xu, X. Jiang, *Chem. Commun.* **2008**, 3642 – 3644.
[25] A study of the growth process of free-standing nanosized $[Cu_3(btc)_2]$ particles (btc = 1,3,5-benzenetricarboxylate) by time-resolved light scattering was recently reported[10].
[26] A. R. Tao, S. Habas, P. Yang, *Small* **2008**, *4*, 310 – 325.
[27] W. W. Yu, Y. A. Wang, X. Peng, *Chem. Mater.* **2003**, *15*, 4300 – 4308.
[28] S. Furukawa, K. Hirai, K. Nakagawa, Y. Takashima, R. Matsuda, T. Tsuruoka, M. Kondo, R. Haruki, D. Tanaka, H. Sakamoto, S. Shimomura, O. Sakata, S. Kitagawa, *Angew. Chem. Int. Ed.* **2009**, *48*, 1766 – 1770.
[29] D. N. Dybtsev, H. Chun, K. Kim, *Angew. Chem. Int. Ed.* **2004**, *43*, 5033 – 5036.
[30] R. Kitaura, F. Iwahori, R. Matsuda, S. Kitagawa, Y. Kubota, M. Takata, T. C. Kobayashi, *Inorg. Chem.* **2004**, *43*, 6522 – 6524.
[31] B.-Q. Ma, K. L. Mulfort, J. T. Hupp, *Inorg. Chem.* **2005**, *44*, 4912 – 4914.
[32] D. Tanaka, M. Higuchi, S. Horike, R. Matsuda, Y. Kinoshita, N. Yanai, S. Kitagawa, *Chem. -Asian J.* **2008**, *3*, 1343 – 1349.
[33] R. L. Penn, J. F. Banfield, *Science* **1998**, *281*, 969 – 971.
[34] J. Polleux, N. Pinna, M. Antonietti, M. Niederberger, *Adv. Mater.* **2004**, *16*, 436 – 439.
[35] N. Pradhan, H. Xu, X. Peng, *Nano Lett.* **2006**, *6*, 720 – 724.

